Growth Anomalies in Supramolecular Networks: 4, 4′-Biphenyldicarboxylic Acid on Cu(001)

Daniel Schwarz,* Raoul van Gastel, Harold J. W. Zandvliet, and Bene Poelsema

Physics of Interfaces and Nanomaterials, MESA+ Institute for Nanotechnology, University of Twente, P. O. Box 217, NL-7500 AE Enschede, The Netherlands

(Received 16 July 2012; revised manuscript received 13 September 2012; published 15 February 2013)

We have used low energy electron microscopy to demonstrate how the interaction of 4, 4′-biphenyldicarboxylic acid (BDA) molecules with (steps on) the Cu(001) surface determines the structure of supramolecular BDA networks on a mesoscopic length scale. Our *in situ* real time observations reveal that steps are permeable to individual molecules but that the change in crystal registry between different layers of the Cu substrate causes them to be completely impermeable to condensed BDA domains. The resulting growth instabilities determine the evolution of the domain shape and include a novel Mullins-Sekerka-type growth instability that is characterized by high growth rates *along*, instead of *perpendicular* to, the Cu steps. This growth instability is responsible for the majority of residual defects in the BDA networks.

DOI: 10.1103/PhysRevLett.110.076101 PACS numbers: 68.35.Rh, 68.37.Nq, 68.43.Jk, 68.55.A−

The growth of metal films on metal substrates has been investigated abundantly in the last decades (e.g., [1–6]). Especially, homoepitaxial growth is understood in great detail [7,8] and its concepts are often used as a benchmark for describing the growth of more complex films, comprised of organic molecules. Those concepts include for instance nucleation behavior and growth instabilities due to kinetic limitations such as restricted edge diffusion and/or mass transport across step edges. In this study, we investigate whether such concepts can guide our understanding of the growth of 2D organic films. For this purpose, we select the growth of 4, 4′-biphenyldicarboxylic acid (BDA) on Cu(001), which represents a timely class of self-assembling 2D hydrogen bonded molecular networks [9–12], particularly those comprised of benzoic acids. The interest lies in their high potential as flexible templates for the fabrication of novel nanoscale structures [13–18]. Much is known about the details of the molecular networks and their building blocks from STM studies [14,15,19–25]. It is, however, remarkable that only a few studies have concentrated on thermodynamic and kinetic aspects of the growth of supramolecular domains on the *mesoscopic* scale [26,27], despite the importance of both to make these networks applicable. The thermodynamic and kinetic aspects become most important for growth under high mobility situations. BDA grows on Cu(001) in a 2D fashion and is therefore excellently suited to compare with (sub)monolayer metal growth. Special attention is paid to differences as a result of binding energy and in particular the shape and size of (large) molecules compared to atoms.

Growth is an inherently statistical process, and this may lead to instabilities known, among others, from metal homoepitaxy. Relevant to the current results is the so-called Mullins-Sekerka (MS) instability [28,29]: Protrusions at steps lead to a locally decreased distance between isoconcentration lines of adatoms and thus enhanced growth, while inclinations lead to the opposite result, a reduction of the growth rate. This generic tendency for instability is counteracted by minimization of step length via edge diffusion and MS defined conditions for its occurrence. For 2D growth, a MS instability leads to enhanced growth *perpendicular* to steps.

In this Letter, we describe how the same concepts that were developed to describe the initial growth of metal films can be applied to understand the growth of molecular films at ''high'' temperature. Low energy electron microscopy (LEEM) and selected area diffraction, or μLEED, were used to study the growth of BDA on Cu(001). BDA is a benzoic acid that deprotonates on Cu(001) below room temperature [14–18]. It consists of two phenyl rings with one functional carboxyl group at each end. The slightly twisted molecule lies flat on Cu(001) and forms a $c(8 \times 8)$ superstructure [16,30], facilitated by a hydrogen bridge between the phenyl groups of one molecule and the carboxylate group of another. A square building block is formed in which adjacent molecules are oriented perpendicularly. LEEM images reveal clear evidence for a MS-type growth instability. We observe the classic case in which an isolated island that is initially compact ramifies during further growth, as well as the classic MS instability at a step. In this case, the growth front moves fastest in a direction perpendicular to the substrate steps. In addition, we demonstrate a not-yet-reported case, in which the growth rate is highest parallel instead of perpendicular to the steps. The latter instability is mainly responsible for deficiencies in the final film.

The experiments have been performed in an Elmitec LEEM III microscope [31] with a base pressure of about 1×10^{-10} mbar. A Cu(001) single crystal with a miscut angle less than 0.1° was used [32]. Prior to mounting, it was annealed at about 1170 K in an Ar-H_2 mixture to deplete the bulk of the crystal from S contamination. The

sample surface was further cleaned in ultrahigh vacuum by cycles of sputtering with hydrogen [33], Ar, and annealing at 900 K. The BDA (purity >0.97, TCI Europe, CAS: 787-70-2) was deposited from a Knudsen cell. The deposition rate was kept constant at 5.1×10^{-4} molecules per nm^2 and per second. In the $c(8 \times 8)$ structure, one molecule occupies 1.04 nm^2. All LEEM images were recorded with 2 eV electrons using a 25 μm illumination aperture and were background corrected by applying a flat field correction. For the surface covered with BDA admolecules, the Cu step contrast is severely reduced. To increase the step contrast, we thus superimposed an image of the clean surface (corrected for image drift) on the LEEM images shown here. Densities of BDA admolecules were estimated from the diffuse reflectivity [34–37]. No indications for electron beam induced damage of the molecular networks were observed at any time. The substrate temperature was kept fixed at 410 K, well below the temperature where thermal decomposition occurs (> 450 K), but also high enough to ensure a very low density of nuclei. No significant desorption of BDA molecules into vacuum takes place, and the condensate is crystalline with a $c(8 \times 8)$ structure at all temperatures [37,38].

In a first experiment, we recorded a LEEM movie (see the Supplemental Material [39]) during deposition of BDA on Cu(001) at 410 K. A few snapshots with a field of view (FoV) of 12 μm are shown in Fig. 1 (top row). The dark gray curved lines represent single steps and step bunches. The bottom panel shows the density of the 2D dilute BDA phase as a function of time. The shutter of the Knudsen cell was opened at $t = 0$ s and closed at 1660 s. The density was measured in the area highlighted by the dashed red circle in the center right-hand image. The "noisy" appearance of the coverage versus time plot is by no means accidental. The first maximum coincides with the first nucleation stage in which two nuclei start to grow within the field of view. Immediately after the growth of the first generation of nuclei, the admolecule density is reduced from the supersaturation that is needed to initiate condensation close to equilibrium [38]. Several observations are immediately evident. First, the number of nuclei is about 2 orders of magnitude lower than the number (~80 within the FoV) of Cu(001) terraces. Second, the consequences of nucleation and growth of new domains affect the admolecule density across at least ten Cu steps over a distance of several microns. Third, secondary nucleation is observed and further nucleation occurs in "waves." Fourth, each combination of a maximum and decay in the admolecule density can be traced down to a single nucleation event. Finally, not all nucleation events become visible in the admolecule density that is measured in the dashed red circle after a prolonged period of nucleation and growth. These observations lead to a number of important conclusions. First, the steps are permeable for individual BDA molecules. A nucleation event on a certain terrace gives rise to variations of the density in the dilute BDA phase on another terrace, separated by ten or more steps. This implies that the Ehrlich-Schwoebel barrier for crossing steps must be low. Second, existing BDA domains act as a high barrier for diffusion of individual BDA molecules, thereby preventing remote nucleation events from becoming visible in the probed area (dashed red circle, top right-hand panel). Third, the steps do not act as preferred nucleation sites since that would lead to roughly one nucleus per terrace and a well-defined nucleation window. Thus, nucleation proceeds through homonucleation rather than heteronucleation. The latter is reiterated by the fact that nuclei eventually emerge on all terraces, and any preference for nucleation at steps is absent.

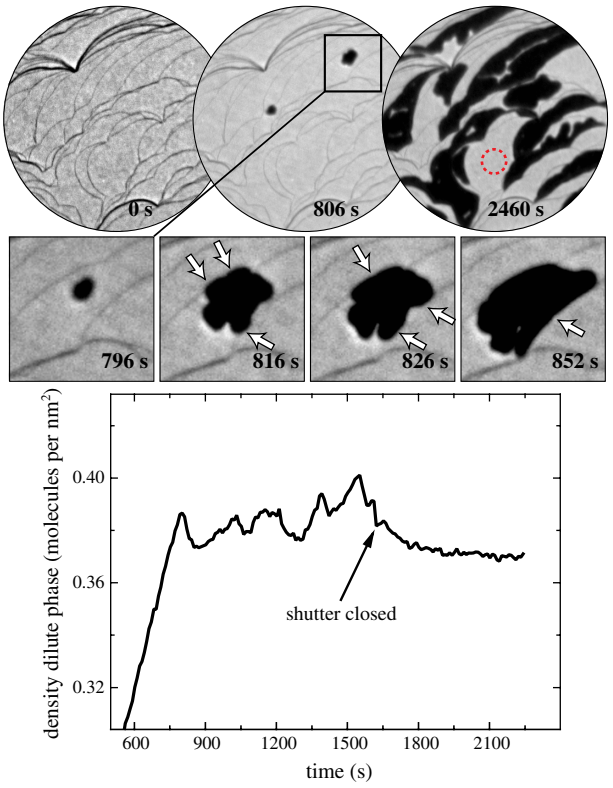

FIG. 1 (color online). Bottom: Coverage in the dilute phase measured in the dashed circle shown in the upper right-hand panel. The BDA deposition was started at $t = 0$ s and stopped at $t = 1660$ s. Nucleation started at 794 s at a dilute phase density of 0.387 molecules per nm^2. Top: Snapshots from a LEEM movie at the indicated times with a FoV of 12 μm. The dark areas correspond to the crystalline $c(8 \times 8)$ structure. The curved lines in the background represent single and multiple steps on the Cu(001) substrate. They are most clearly visible for the clean substrate and to increase step contrast; we added the first image to the subsequent LEEM images, also in the further figures (see also the text). Center: The growth of a single BDA domain. First, a compact shape develops, which evolves into a ramified one with protrusions and recesses due to a MS growth instability. Upon further growth, the protrusions hit the Cu step first (arrows). Recesses remain, which are subsequently filled until the domain edges precisely follow the steps bordering the host terrace.

The subsequent waves of nucleation events, as illustrated in Fig. 1 (bottom panel), are unexpected at first sight. In classic nucleation and growth, the few initial nuclei (density ≈ 0.009 per μm^2) would continuously grow until the complete area is filled, provided that the steps are permeable for individual BDA molecules. This situation, however, does not apply here. The Cu steps apparently provide a highly efficient way to terminate aggregation beyond steps. This is easily understood: Except for a potentially inhibiting height difference of about 2.08 Å per Cu step, the fcc structure of Cu imposes also a registry problem. The $c(8 \times 8)$ registry is shifted by at least half a nearest-neighbor distance in two $\langle 110 \rangle$ directions on terraces that are separated by a single step. Therefore, already single steps impede the aggregation of BDA domains. Consequently, steps act as effective terminators for BDA domains, even when individual molecules can easily pass them. This implies that, when a significant fraction of domain boundaries is impinging on steps, further aggregation of BDA molecules is suppressed and the admolecule density rises again, repeatedly leading to a new nucleation wave until eventually all terraces are filled. The $c(8 \times 8)$ structure has 32 equivalent translational domains. In order to minimize the number of different domains in a network, the initial number of nuclei has to be well below the number of Cu terraces, as is the case in Fig. 1. One single domain will then develop on each terrace. However, macroscopically, all variations will occur.

We now inspect the influence of the steps in more detail. Figure 2 shows a LEEM image that was recorded 800 s after closing the shutter of the Knudsen cell (cf. Fig. 1). It reveals a contact angle of the condensate with the Cu steps that is well above 150°. This observation is very significant. In three dimensions, the contact angle ϕ between a substrate and a film is given by Young's equation:

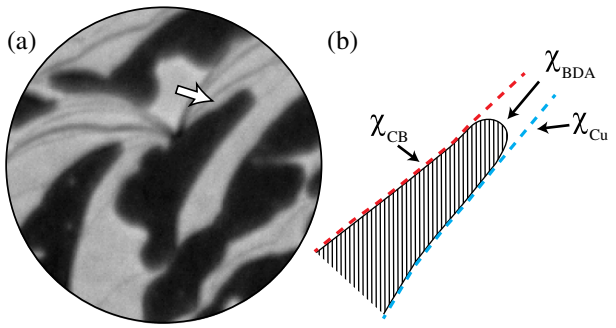

FIG. 2 (color online). (a) LEEM image (FoV = 6 μm) taken 800 s after closing the shutter. The dark areas represent $c(8 \times 8)$ crystallites. The bright spots inside the domains are vacancy clusters that have reduced their edge lengths after coalescence (see Fig. 1). (b) Sketch of the region indicated by the arrow in (a). The dashed lines indicate descending (red, darker gray) and ascending (blue, light gray) steps. χ_{CB}, χ_{BDA} and χ_{Cu} indicate the line tensions for the BDA covered step, the BDA domain boundary, and the uncovered Cu step, respectively.

$$\cos\phi = \frac{\sigma_s - \sigma_i}{\sigma_f}, \tag{1}$$

where σ_s, σ_i, and σ_f refer to the surface tension of the substrate, the interface, and the film, respectively. In the present two-dimensional case, these are replaced by the line tensions of the free Cu step, the BDA covered Cu step, and the BDA domain, respectively. A small value for ϕ is indicative for strong adhesion and wetting of the steps by BDA, while large ϕ values reveal a weak interaction and nonwetting. It is obvious from inspection of Fig. 2 that there is strong nonwetting, which is consistent with the observation that steps do not act as nucleation centers. The latter is already indicative of a low affinity to the steps. The island expansion is terminated by the steps, i.e., when no additional BDA molecule fits in between the step and the $c(8 \times 8)$ edge. So, most islands will not even make physical contact to the step.

The growth of BDA/Cu(001) exhibits several instabilities, which we now consider in more detail. First, we examine an early stage of growth, as depicted in the second snapshot in the top panel of Fig. 1. It shows two nuclei that are compact. A more detailed inspection of the evolution of the right domain is shown in the center panel. Protrusions develop that evolve into a ramified shape. This behavior is characteristic of a Mullins-Sekerka growth instability: Protrusions capture material from an area with a larger solid angle. This behavior is common to all growing islands, as discussed in the Supplemental Material [39]. In the BDA/Cu(001) system, the protrusions will be strongly enhanced because the mobility along the edges of BDA domains is extremely low. Edge molecules are alternatingly placed in an orientation perpendicular and parallel to the edge along the $\langle 110 \rangle$ directions, as shown in Fig. 3. Movement along such edges involves detachment, diffusion in the vicinity of the edge, and reattachment at an appropriate position. For ideal $\langle 110 \rangle$ oriented edges, an additional rotation of the molecule in the disordered "gas" phase is required. Along a perfect $\langle 100 \rangle$ oriented step, all molecules are oriented parallel. A diffusing molecule will only have parallel binding partners and be weakly bound, while reattachment requires a rotation of the molecule in the dilute phase. In either case, mass transport along the BDA domain edges will be slow and the MS instability criterion is therefore well met. In more advanced stages of growth, protrusions of the domain will impinge on steps (see the arrows in Fig. 1) where further growth is inhibited. The final result is that all domain boundaries impinge on steps and follow the smooth contour of the step. Figure 4 presents the shape evolution of the BDA island shown in the center panel of Fig. 1. Each color represents the island shape after an incremental 20 s. If we concentrate on the growth along the right-hand side of the lower Cu step, we can see that the domain growth rate is very fast, much faster than the growth rate away from the step toward the terrace (cf. the red arrows in Fig. 4). For the

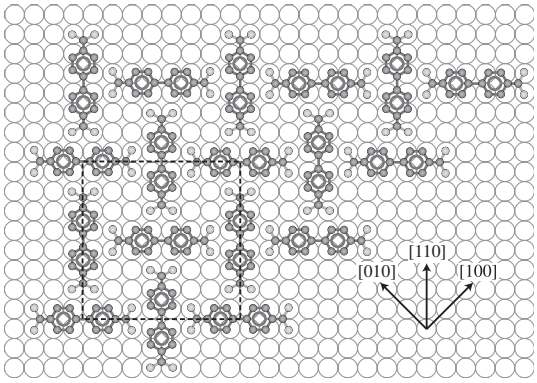

FIG. 3. A sketch of the BDA molecules in the $c(8 \times 8)$ structure, with the unit cell shown by the dashed square. The crystallographic azimuth directions on Cu(001) are shown in the inset.

growing domain front at the step, the solid angle for accepting incoming admolecules is over 270°. Note that the steps are permeable for individual admolecules. For the material arriving within the remaining 90°, the front competes with domain boundaries further toward the interior. The solid angle that is available for diffusing species is thus very large, which can result in extremely fast growth. Even at a very low deposition rate of 5.1×10^{-4} molecules $\mathrm{nm}^{-2}\,\mathrm{s}^{-1}$, domain boundary growth rates of 40–100 nm/s have been observed. The very different growth rates may even result in the formation of vacancy clusters (cf. the white arrow in Fig. 4). Clearly, this growth instability fulfills all requirements of a MS growth instability. The edge mobility is still extremely low, as explained above, while the accumulation

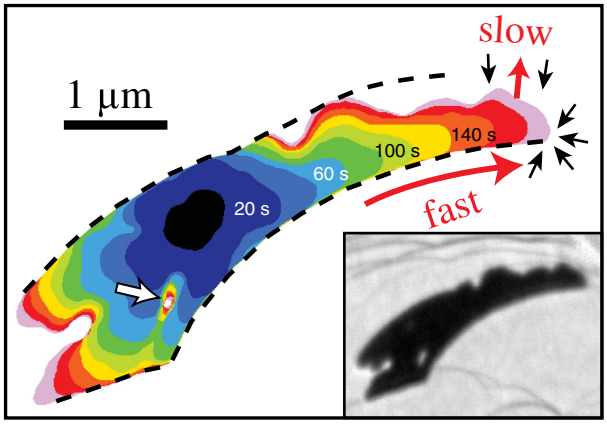

FIG. 4 (color online). Color coded shape evolution of the island shown in the center panel of Fig. 1. Each color represents the island shape after a time increment of 20 s. The dotted lines indicate the bordering Cu steps. The fast growth *along* steps can be seen at the right-hand side of the lower step. The conventional MS instability can be seen for the much slower growth *away* from the step. Red (gray) arrows indicate the domain expansion rate, black arrows the BDA admolecule flux. The white arrow marks the inclusion of a vacancy hole. The inset shows a LEEM image of the island at the latest stage.

of isoconcentration lines around the protrusion is extremely high. The latter is enhanced by the fact that the surrounding BDA domain boundaries are no longer able to accommodate BDA molecules because they are limited by the Cu steps. Counterintuitively, the fast growth direction is, however, along the step, instead of the more common direction perpendicular to the steps. This unexpected growth behavior is a direct consequence of the underlying physics: a non- or only weak wetting of steps. It should be of general importance for a wide range of molecular film systems, in which the affinity of molecules for steps is low. The high growth rate along the steps leads eventually to the pinching off of vacancy holes after the coalescence of the growing "fingers." Each completed domain will have several of these holes; cf. Fig. 1 and the LEEM images in the Supplemental Material [39].

We have reported anomalous growth features for BDA/Cu(001), representing the important class of benzoic acid networks on metal substrates. We find strong MS-type instabilities: the ramification of initially compact islands and a yet unknown type of MS instability, characterized by the fast growth rate of islands along preexisting Cu steps. This fact, together with the applicability of nucleation theory [38], lets us conclude that an interesting and important regression of concepts from atomic scale growth to molecular systems can be inferred. However, caution is required when contemplating a rigorous application of atomic concepts for the growth of molecular films. For instance, the size of the molecules, adsorbed on fcc Cu(001), is directly responsible for the termination of the domain growth by steps. The role of steps, both as diffusion barriers and preferred nucleation sites, is likely less pronounced than in metal epitaxy.

The present findings are highly relevant for the improved fabrication of 2D molecular layers. The best condition for defect-free domains is found at high temperature or better for low E_D/kT values, warranting only one nucleus per terrace. E_D is the activation barrier for diffusion. This avoids the evolution of multiple translational domains and the corresponding boundary defects. The evolution of translational domains is a natural consequence of large molecules: not less than 32 are possible for BDA/Cu(001). Note that Ostwald ripening is highly ineffective for domains of similar size. More importantly, line defects are very persistent even in metal films where they anneal only at high temperature. For molecular films, the required temperature budget may not be available due to the finite thermal stability of the building blocks.

*Present address: Peter Grünberg Institut (PGI-3), Forschungszentrum Jülich, 52425 Jülich, Germany and Jülich Aachen Research Alliance (JARA)-Fundamentals of Future Information Technology, 52425 Jülich, Germany.

[1] H. Brune, Surf. Sci. Rep. **31**, 125 (1998).
[2] B. Poelsema, R. Kunkel, N. Nagel, A. F. Becker, G. Rosenfeld, L. K. Verheij, and G. Comsa, Appl. Phys. A **53**, 369 (1991).
[3] M. Bott, T. Michely, and G. Comsa, Surf. Sci. **272**, 161 (1992).
[4] T. Michely, M. Hohage, M. Bott, and G. Comsa, Phys. Rev. Lett. **70**, 3943 (1993).
[5] G. Rosenfeld, B. Poelsema, and G. Comsa, J. Cryst. Growth **151**, 230 (1995).
[6] P. Gambardella, M. Blanc, L. Bürgi, K. Kuhnke, and K. Kern, Surf. Sci. **449**, 93 (2000).
[7] T. Michely and J. Krug, *Islands, Mounds and Atoms*, edited by G. Ertl, H. Lüth, and D. L. Mills (Springer-Verlag, Berlin, 2004), 1st ed.
[8] J. W. Evans, P. A. Thiel, and M. C. Bartelt, Surf. Sci. Rep. **61**, 1 (2006).
[9] D. Philp and J. F. Stoddart, Angew. Chem., Int. Ed. Engl. **35**, 1154 (1996).
[10] G. Whitesides, J. Mathias, and C. Seto, Science **254**, 1312 (1991).
[11] O. Ivasenko and D. F. Perepichka, Chem. Soc. Rev. **40**, 191 (2010).
[12] A. Langner, S. L. Tait, N. Lin, R. Chandrasekar, V. Meded, K. Fink, M. Ruben, and K. Kern, Angew. Chem., Int. Ed. Engl. **51**, 4327 (2012).
[13] J. K. Gimzewski and C. Joachim, Science **283**, 1683 (1999).
[14] A. Dmitriev, N. Lin, J. Weckesser, J. V. Barth, and K. Kern, J. Phys. Chem. B **106**, 6907 (2002).
[15] S. Stepanow, T. Strunskus, M. Lingenfelder, A. Dmitriev, H. Spillmann, N. Lin, J. V. Barth, Ch. Wöll, and K. Kern, J. Phys. Chem. B **108**, 19 392 (2004).
[16] S. Stepanow, N. Lin, F. Vidal, A. Landa, M. Ruben, J. V. Barth, and K. Kern, Nano Lett. **5**, 901 (2005).
[17] M. Lackinger and W. M. Heckl, Langmuir **25**, 11 307 (2009).
[18] J. V. Barth, Surf. Sci. **603**, 1533 (2009).
[19] S. Clair, S. Pons, A. P. Seitsonen, H. Brune, K. Kern, and J. V. Barth, J. Phys. Chem. B **108**, 14 585 (2004).
[20] T. Classen, M. Lingenfelder, Y. Wang, R. Chopra, C. Virojanadara, U. Starke, and G. Costantini, J. Phys. Chem. A **111**, 12 589 (2007).
[21] A. Langner, S. L. Tait, N. Lin, C. Rajadurai, M. Ruben, and K. Kern, Proc. Natl. Acad. Sci. U.S.A. **104**, 17 927 (2007).
[22] M. Ruben, D. Payer, A. Landa, A. Comisso, C. Gattinoni, N. Lin, J.-P. Collin, J.-P. Sauvage, A. De Vita, and K. Kern, J. Am. Chem. Soc. **128**, 15 644 (2006).
[23] S. Stepanow, M. Lingenfelder, A. Dmitriev, H. Spillmann, E. Delvigne, N. Lin, X. Deng, C. Cai, J. V. Barth, and K. Kern, Nat. Mater. **3**, 229 (2004).
[24] M. E. Cañas Ventura, F. Klappenberger, S. Clair, S. Pons, K. Kern, H. Brune, T. Strunskus, Ch. Wöll, R. Fasel, and J. V. Barth, J. Chem. Phys. **125**, 184710 (2006).
[25] W. D. Xiao, Y. H. Jiang, K. Aït-Mansour, P. Ruffieux, H.-J. Gao, and R. Fasel, J. Phys. Chem. C **114**, 6646 (2010).
[26] J. V. Barth, G. Costantini, and K. Kern, Nature (London) **437**, 671 (2005).
[27] J. Ikonomov, C. H. Schmitz, and M. Sokolowski, Phys. Rev. B **81**, 195428 (2010).
[28] W. W. Mullins and R. F. Sekerka, J. Appl. Phys. **34**, 323 (1963).
[29] W. W. Mullins and R. F. Sekerka, J. Appl. Phys. **35**, 444 (1964).
[30] F. S. Khokhar, R. van Gastel, D. Schwarz, H. J. W. Zandvliet, and B. Poelsema, J. Chem. Phys. **135**, 124706 (2011).
[31] E. Bauer, Rep. Prog. Phys. **57**, 895 (1994).
[32] U. Linke and B. Poelsema, J. Phys. E **18**, 26 (1985).
[33] R. Bouwman, J. Vac. Sci. Technol. **15**, 91 (1978).
[34] J. de la Figuera, N. C. Bartelt, and K. F. McCarty, Surf. Sci. **600**, 4062 (2006).
[35] E. Loginova, N. C. Bartelt, P. J. Feibelman, and K. F. McCarty, New J. Phys. **10**, 093026 (2008).
[36] E. Loginova, N. C. Bartelt, P. J. Feibelman, and K. F. McCarty, New J. Phys. **11**, 063046 (2009).
[37] D. Schwarz, R. van Gastel, H. J. W. Zandvliet, and B. Poelsema, Phys. Rev. B **85**, 235419 (2012).
[38] D. Schwarz, R. van Gastel, H. J. W. Zandvliet, and B. Poelsema, Phys. Rev. Lett. **109**, 016101 (2012).
[39] See Supplemental Material at http://link.aps.org/supplemental/10.1103/PhysRevLett.110.076101 for an analysis of the domain circularity versus size and a LEEM movie showing the BDA domain growth.